

Long-range fluctuations of random potential landscape as a mechanism of $1/f$ noise in hydrogenated amorphous silicon

Boris V. Fine*

*Max Planck Institute for the Physics of Complex Systems, Noethnitzer Str. 38, D-01187
Dresden, Germany*

and

Spinoza Institute, P.O. Box 80195, 3508 TD Utrecht, The Netherlands

Jeroen P. R. Bakker and Jaap I. Dijkhuis

Debye Institute, Utrecht University, P.O. Box 80000, 3508 TA Utrecht, The Netherlands

Received (received date)

Revised (revised date)

Accepted (accepted date)

We describe a mechanism, which links the long-range potential fluctuations induced by charged defects to the low frequency resistance noise widely known as $1/f$ noise. This mechanism is amenable to the first principles microscopic calculation of the noise spectrum, which includes the absolute noise intensity. We have performed such a calculation for the thin films of hydrogenated amorphous silicon (a-Si:H) under the condition that current flows perpendicular to the plane of the films, and found a very good agreement between the theoretical noise intensity and the measured one. The mechanism described is quite general. It should be present in a broad class of systems containing poorly screened charged defects.

Keywords: $1/f$ noise, long-range potential fluctuations, amorphous silicon

1. Introduction

In this work we present a theoretical and experimental study of low-frequency voltage noise in μm -thick films of amorphous silicon (a-Si:H) under the condition that electric current flows perpendicularly to the plane of the films. This phenomenon is associated with resistance fluctuations, which, in the presence of current, manifest themselves as voltage noise. The spectrum of this noise is close to $1/f$, where f is the frequency.

Our motivation for this work is two-fold. On the one hand, we describe a new microscopic mechanism of $1/f$ noise, which should be present in a variety

*Present address of B. V. F.: Physics Department, University of Tennessee, 1413 Circle Dr., Knoxville, TN 37996, USA. E.mail:bfine@utk.edu

of systems. On the other hand, the particular material studied, a-Si:H, is very important technologically because of its applications in various photo-voltaic devices (such as e.g. solar cells and thin-film transistors). The technological importance of a-Si:H represents the further advantage, that this material has been heavily studied in the past, and, therefore, its microscopic characteristics, which we need as input to our theory, are reasonably well known [1].

Among many existing proposals aimed at the general description of $1/f$ noise, perhaps, the most successful one is the model of an ensemble of two-state systems having a broad distribution of activation energies (BDAE) [2–4]. The BDAE model gives a reasonable explanation for the generic nature of spectral shapes close to $1/f$ and, furthermore, (after Dutta, Dimon and Horn [4]) predicts the temperature dependence of the small deviations from that shape. It is the experimental observation of those small deviations in a variety of systems [5] that constitutes the strongest evidence for the adequacy of the BDAE model. However, this model as such does not represent a full theoretical description of the noise, because it does not address the origin of the two-state systems and the mechanism by which they couple to the resistance fluctuations. As a result, the absolute intensity of the $1/f$ noise remains an adjustable parameter.

In principle, it is not obvious at all that a universal mechanism should underlie every occurrence of $1/f$ noise in the systems, that seem to obey the BDAE description. However, the unsatisfactory reality is that there are no examples (at least, we are not aware of any), when a microscopic mechanism of the $1/f$ noise has been worked out in full detail for one “BDAE” system, and, at the same time, the results of the calculation based on that mechanism have agreed with experiment. Here “full detail” means: (i) the identification of microscopic fluctuators with their activation energies and activation rates; (ii) identification of the mechanism that couples those fluctuators to the resistance noise; and (iii) a first principles calculation of the absolute noise intensity. Such a “full detail” treatment was recently given by us for a-Si:H in Ref. [6]. This treatment, however, included many material-specific details, not all of which were crucially important for the understanding the noise mechanism. In this work, we describe the same experimental setting as in Ref. [6] but do so in a more intuitive way by replacing some detailed calculations with simple estimates. It turns out that the outcome of such a description is not much different from that of the full calculation.

2. Film characteristics and experimental details.

We study an $n - i - n$ film of a-Si:H, where n denotes an electron doped layer, and i an undoped layer. The thickness of each of the n -layers is 40 nm, while the thickness of the i -layer is $d = 0.91\mu\text{m}$. The area of the film is $A = 0.56\text{cm}^2$. The film was grown by plasma enhanced chemical vapor deposition (PECVD). It was subsequently thermally annealed and, afterwards, kept protected from light. The setup of our noise experiments was the same as in Ref. [7].

We observed voltage noise spectra at frequencies $f = 1 \div 10^4$ Hz and temperatures $T = 340 \div 434$ K in the presence of electric current flowing perpendicularly to the plane of the film. The film itself was thus sandwiched between highly conductive contact layers. The voltages applied were small enough to correspond to

the linear part of the film's I-V characteristic. The experiments were performed without illumination of the film.

3. Previous studies of $1/f$ noise in a-Si:H

The previous studies of $1/f$ noise in the films of a-Si:H [7–16] illustrate the general situation described in Section 1: although a large body of diverse phenomenological information about the noise has been collected, the problem of identifying the origin of the noise has remained open.

In this work we focus only on one out of many possible situations that have been studied experimentally: perpendicular current, no illumination, undoped main resistivity layer, annealed sample. In that case, it was shown experimentally [7] that (i) the statistics of noise is Gaussian and (ii) the temperature dependence of the spectral slope (parametrizing the small deviations from the exact $1/f$ dependence) agrees well with the BDAE model.

It was evident since the early studies [8], that the timescales of activation for the electron escape from deep defects in a-Si:H correspond well to the frequency range where the noise was observed. The problem was that, even though the energies of the defect levels have a relatively broad distribution, the Fermi factor limits the noise to the levels, which are located in the thermal window around the chemical potential [9]. This thermal window is not broad enough to give a spectral shape close to $1/f$.

If, nevertheless, one insists on computing the noise intensity associated with the fluctuations of the defect occupation numbers, then there are still two general scenarios: the resistance fluctuations can be due to the fluctuations of either the number of free carriers or their mobility. The fluctuations of the number of free carriers can be produced by the random emission and capture of free electrons by deep defects. This possibility was investigated by Verleg and Dijkhuis [7] (albeit on the basis of a very simple model). They came to conclusion that the noise intensity due to this mechanism would be several orders of magnitude smaller than the one observed, and, furthermore, the timescale of such a noise would be controlled by the fast capture times rather than the slow emission times, which shifts the characteristic noise frequency away from the observation range. Later, a more detailed theoretical investigation of this type of noise has supported the conclusion of a low noise intensity [17].

A simple realization of mobility fluctuations could be related to the change of the defect cross-sections. This scenario, however, has the problem that the relative concentration of deep defects is too small to affect the transport of free carriers. The mobility of free carriers is controlled mainly by the elastic scattering from the short-range inhomogeneities of the amorphous lattice structure.

Other mechanisms of the $1/f$ noise in a-Si:H have also been proposed, including thermally activated chemical processes [9], generation-recombination processes with various degrees of sophistication [7, 13, 18], and, finally, resistance networks near percolation threshold [19] (in the context of coplanar currents).

Although, in principle, each of these proposals can be viable, none of them has been tested conclusively so far.

4. Outline of the noise mechanism proposed in this work

In the following, we shall revive the old idea that the noise is caused by the fluctuations of the defect occupation numbers. That idea, however, is complemented by a novel noise mechanism, which involves long-range potential fluctuations induced by fluctuations of the defect charges. These potential fluctuations then cause the fluctuations of the local densities of conduction electrons, which, in turn, lead to the observed resistance fluctuations.

It is important to realize that the above mechanism should certainly be present in the material studied. Its theoretical description is quite straightforward and, at the same time, gives the value of integrated noise intensity without adjustable parameters. Therefore, if such a theory produces the noise intensity comparable with the one observed in experiment, then it is quite unlikely that another noise mechanisms contributes to the experimental spectrum on the top of the one just described.

Our theoretical description also contains a new, though very simple, idea that the distribution of the fluctuation rates of defect charges comes not just from the distribution of the energy levels of electrons bound to the defects, but also from the distribution of the activation barriers, which electrons have to overcome to escape from the defects. Unlike the former distribution, the later one is not truncated by the Fermi factor [5, 9] and thus can underlie the spectral shape close to $1/f$.

In the rest of this paper, our theory is exposed in Sections 5-9 followed by comparison with experiments (Section 10) and conclusions(Section11). Central to our treatment is Section 7, which contains the description of the noise mechanism.

5. Quantity of interest

The voltage noise spectrum can be expressed as:

$$\frac{S_V(f)}{V^2} = 4 \int_0^\infty C_V(t) \cos(2\pi ft) dt, \quad (1)$$

where V is the applied voltage, and

$$C_V(t) = \frac{\langle \delta V(t) \delta V(0) \rangle}{V^2} = \frac{\langle \delta R(t) \delta R(0) \rangle}{R_0^2}. \quad (2)$$

Here, $\delta V(t)$ is the voltage fluctuation, R_0 is the average resistance of the film, and $\delta R(t)$ is the equilibrium resistance fluctuation.

The second equality in Eq.(2) follows from the assumption of constant current I flowing through the film, i.e. $\delta V(t) = I \delta R(t)$ and $V = IR_0$. The assumption of constant current is granted, because (i) the current noise of external origin is suppressed by a very large resistance connected in series with the film; and (ii) the current noise of "internal" origin manifests itself at the equilibrium Johnson-Nyquist noise [20, 21], which was measured independently with zero applied voltage and then subtracted from the spectrum taken with non-zero voltage.

The link between the resistance noise and the voltage noise has also been established experimentally by observing that $S_V(f)$ defined as the difference between the spectra at zero applied voltage and non-zero applied voltage is proportional to V^2 .

6. Description of the resistivity layer

In the following, we consider a somewhat idealized problem of resistance noise coming from a resistivity layer of thickness z_r and volume $V_r = z_r A$ having uniform material characteristics. Because of the band bending, most of the resistance of our actual film originates from the center of the intrinsic layer. The effective thickness of that central layer is [6] $z_r = 0.26 \mu\text{m}$.

The density of states of undoped a-Si:H is characterized by a band gap of 1.8 eV between the mobility edges E_v and E_c in the valence and conduction bands, respectively. The defect states, which play an important role in the noise mechanism, are located deep inside the band gap. Because of the proximity of the n-layers, the chemical potential μ is significantly closer to E_c than to E_v . (From the measurements of the conductivity activation energy, we estimate that $E_c - \mu = 0.63 \text{ eV}$.) As a result, the number of electrons in the conduction band is much greater than the number of holes in the valence band, i.e. conduction electrons are the primary carriers of electric current.

One parameter, which is particularly important for the rest of this work, is r_s , the screening radius of deep defects. In order to estimate it, we first note that the conventional mechanism of screening by conduction electrons is not operational in our film, because, at the temperatures of experiment, their concentration ($10^{10} - 10^{13} \text{ cm}^{-3}$) is much smaller than the concentration of deep defects ($\sim 10^{16} \text{ cm}^{-3}$). Instead, we identify two screening mechanisms: (i) by contact layers and (ii) by other deep defects. The effective screening radius due to both screening mechanisms was estimated in Ref. [6] as $0.2 \mu\text{m}$.

In order to simplify the theoretical description, we shall assume that $r_s \ll z_r$, i.e., in this sense, we consider three-dimensional ‘‘bulk’’ limit. In our film, $r_s \sim z_r$. However, the noise intensity computed with the actual values of r_s and z_r differs from the outcome of the bulk limit calculation only by factor of two [6].

We also assume that the film is still thin enough, so that an electron emitted from a deep defect is much more likely to escape into the contact layers than to be captured by another deep defect. This means that the charges of different deep defects fluctuate independently. Such an assumption is well applicable to the experiments with transverse currents [6], because, in these experiments, the contact layers spread over the entire film surface, which means that any defect in the resistivity layer is no more than half of the film thickness away from the contacts. However, the same assumption is not applicable to the experiments with co-planar currents [10–12, 14, 16, 22, 23], where the distance to contacts is of the order of the in-plane dimensions of the films.

7. Relation between the resistance fluctuations and the long-range fluctuations of the local potential

Now we describe the fluctuations of the resistivity within the resistivity layer. These fluctuations arise as a consequence of the fluctuations of the screened Coulomb potential $\phi(t, \mathbf{r})$ created by deep charged defects, known as dangling bonds:

$$\phi(t, \mathbf{r}) = \sum_i \frac{\Delta q_i(t)}{\epsilon |\mathbf{r} - \mathbf{a}_i|} \exp\left(-\frac{|\mathbf{r} - \mathbf{a}_i|}{r_s}\right). \quad (3)$$

Here $\Delta q_i(t)$ is the fluctuation of the i th defect charge with respect to its average value, \mathbf{a}_i the position the defect, r_s the screening radius, and $\epsilon = 12$ the dielectric constant. The defects involved may be located outside of the resistivity layer.

When the potential $\phi(t, \mathbf{r})$ fluctuates, the mobility edge tracks it, i.e.

$$E_c(t, \mathbf{r}) = E_{c0} + e\phi(t, \mathbf{r}), \quad (4)$$

where e is the electron charge. Since the chemical potential μ does not shift with $e\phi(t, \mathbf{r})$, the density of conduction electrons, n_e , re-equilibrates following $E_c(t, \mathbf{r})$ on the timescale of electron drift from the center of the i -layer to the n -layers. Because of the strong band bending inside the i -layer [6], the drift takes less than 10^{-7} s, i.e. the re-equilibration is effectively instantaneous on the timescales of the noise studied ($\frac{2\pi}{f} \sim 10^{-4} \div 1$ s). The fluctuating quasi-equilibrium density of the conduction electrons is then proportional to $\exp[-(E_c(t, \mathbf{r}) - \mu)/k_B T]$, where k_B is the Boltzmann constant. Finally, the fluctuating local resistivity ρ , which is inversely proportional to n_e , can be written as

$$\rho(t, \mathbf{r}) = X \exp\left(\frac{E_c(t, \mathbf{r}) - \mu}{k_B T}\right), \quad (5)$$

where X is a proportionality coefficient.

Assuming for a moment [and proving later] that

$$|e\phi(t, \mathbf{r})| \ll k_B T, \quad (6)$$

we expand

$$\rho(t, \mathbf{r}) = \rho_0 + \delta\rho(t, \mathbf{r}), \quad (7)$$

where

$$\rho_0 = X \exp\left(\frac{E_{c0} - \mu}{k_B T}\right), \quad (8)$$

and

$$\delta\rho(t, \mathbf{r}) = \frac{e\phi(t, \mathbf{r})}{k_B T} \rho_0. \quad (9)$$

For $\delta\rho \ll \rho_0$, the fluctuation of the total resistance (derived in the Appendix) is

$$\delta R(t) = \frac{1}{A^2} \int_{\mathcal{V}} \delta\rho(t, \mathbf{r}) d^3 r, \quad (10)$$

where \mathcal{V} is the space inside the resistivity layer (limited by $\pm z_r/2$ along the z -axis and by the edges of the film in the xy -plane). Substituting $R_0 = z_r \rho_0 / A$ and $\delta R(t)$ given by Eq.(10) into Eq.(2), and then using Eq.(9), we obtain

$$C_V(t) = \left(\frac{e}{k_B T V_r}\right)^2 \int_{\mathcal{V}} d^3 \mathbf{r} \int_{\mathcal{V}} d^3 \mathbf{r}' \langle \phi(t, \mathbf{r}) \phi(0, \mathbf{r}') \rangle. \quad (11)$$

Given Eq.(3), the correlation function of potential fluctuations can be written as

$$\langle \phi(t, \mathbf{r}) \phi(0, \mathbf{r}') \rangle = \sum_{i,j} \frac{\langle \Delta q_i(t) \Delta q_j(0) \rangle}{\epsilon^2 |\mathbf{r} - \mathbf{a}_i| |\mathbf{r}' - \mathbf{a}_j|} \exp\left[-\frac{|\mathbf{r} - \mathbf{a}_i| + |\mathbf{r}' - \mathbf{a}_j|}{r_s}\right] \quad (12)$$

Equation (11) should have a very broad range of applicability. All the material-specific details affect only the evaluation of $\langle \phi(t, \mathbf{r}) \phi(0, \mathbf{r}') \rangle$. In Ref. [6], we have performed this evaluation taking into account numerous microscopic characteristics of a-Si:H. Below, however, we present a cruder estimate, which is more intuitive and yet reasonably accurate.

The time dependence of $\langle \phi(t, \mathbf{r}) \phi(0, \mathbf{r}') \rangle$ in Eq.(12) comes from the correlators of charge fluctuations $\langle \Delta q_i(t) \Delta q_j(0) \rangle$. For $i \neq j$, $\langle \Delta q_i(t) \Delta q_j(0) \rangle = 0$, because, as discussed in Section 6, the charge fluctuations of different defects are independent of each other. The non-zero contribution comes from the correlators with $i = j$, which can be expressed as

$$\langle \Delta q_i(t) \Delta q_i(0) \rangle = \langle \Delta q_i^2 \rangle \exp\left(-\frac{t}{\tau_i}\right). \quad (13)$$

Here $1/\tau_i$ is the fluctuation rate of the i th defect. The correlator is characterized by a single exponent, because every defect is assumed to have only two states neutral or charged (with charge either $+e$ or $-e$). The potential fluctuations are induced mainly by the defects, which we call ‘‘thermally active’’ or simply ‘‘active.’’ These active defects have binding energies E in the thermal window $\pm 2k_B T$ around the chemical potential μ . Their concentration is, therefore,

$$n_T = 4 k_B T D(\mu), \quad (14)$$

where $D(\mu)$ is the density of defect states around the chemical potential. It can be estimated as

$$D(\mu) = \frac{n_D}{2\Delta E}, \quad (15)$$

where n_D is the total concentration of deep defects, and ΔE is the half-width of the distribution of their binding energies. We have found that in our film [6] $n_D \approx 6 \cdot 10^{15} \text{ cm}^{-3}$, and $\Delta E \approx 0.15 \text{ eV}$.

In comparison with the rest of the defects, the thermally active ones have the largest amplitude of charge fluctuations. The absolute value of their charge has roughly the same probability to be 0 or e . Therefore, its mean value is $e/2$, and the mean squared amplitude of fluctuations is

$$\langle \Delta q_T^2 \rangle \approx \frac{e^2}{4}. \quad (16)$$

Now we estimate $\langle \phi(t, \mathbf{r}) \phi(0, \mathbf{r}') \rangle$ by taking the average over the spatial distribution of active defects (assumed to be random) and over the distribution of their relaxation times (inverse fluctuation rates) $P_\tau(\tau)$. For this estimate we use the following *Ansatz*:

$$\langle \phi(t, \mathbf{r}) \phi(0, \mathbf{r}') \rangle = \langle \phi^2 \rangle \exp\left[-\frac{|\mathbf{r} - \mathbf{r}'|}{r_s}\right] \int \exp\left(-\frac{t}{\tau}\right) P_\tau(\tau) d\tau, \quad (17)$$

where, from Eqs.(12,14,16),

$$\langle \phi^2 \rangle \equiv \langle \phi(0, 0)^2 \rangle = \int \frac{\langle \Delta q_T^2 \rangle}{\epsilon^2 r''^2} \exp\left(-\frac{2r''}{r_s}\right) n_T 4\pi^2 r''^2 dr'' = \frac{2\pi e^2 r_s D(\mu) k_B T}{\epsilon^2}, \quad (18)$$

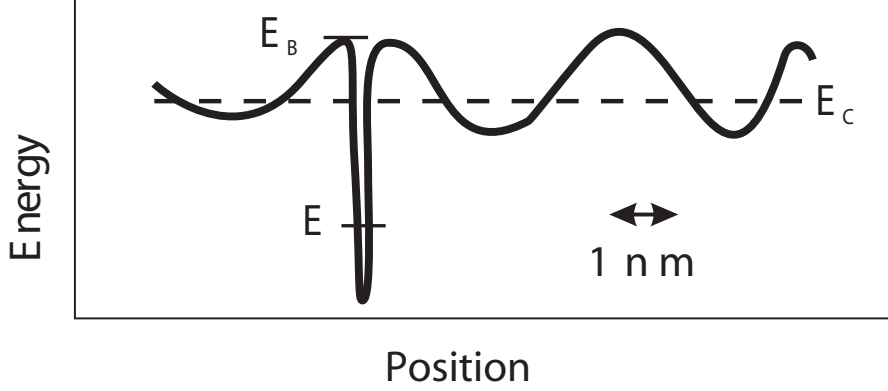


Fig 1. Cartoon of a deep defects surrounded by medium-range structural disorder. Note: $e\phi(t, \mathbf{r})$ fluctuates on a much longer length scale and with much smaller amplitude.

where r'' is an integration variable corresponding to $|\mathbf{r} - \mathbf{a}_i|$ in Eq.(12). From Eq.(18), the value of $|e\phi(t, \mathbf{r})|$ can be estimated as: $e\sqrt{\langle\phi^2\rangle} \sim 3.5\text{meV}$. Since $k_B T \sim 30\text{meV}$, the assumption (6) was adequate.

Substituting Eqs.(17,18) into Eq.(11) and integrating over \mathbf{r} and \mathbf{r}' (under the assumption $r_s \ll z_r$ made in Section 6), we obtain

$$C_V(t) = \frac{16\pi^2 e^4 r_s^4 D(\mu)}{\epsilon^2 k_B T V_r} \int \exp\left(-\frac{t}{\tau}\right) P_\tau(\tau) d\tau. \quad (19)$$

Now we discuss the origin of the distribution of the activation times $P_\tau(\tau)$.

8. Activation barriers

In order to escape from a deep defect, an electron should reach the mobility edge E_c . However, the activation barriers E_B (indicated in Fig.1) can vary as a result of the *medium-range* disorder of the amorphous structure (on a length scale of $1 \div 10 \text{ nm}$). The activation time of a thermally active defect should then read

$$\tau(E_B) = \tau_0 \exp\left(\frac{E_B - \mu}{k_B T}\right), \quad (20)$$

where τ_0 is the prefactor of the order of 10^{-13} s [6].

In Ref. [6], we have assumed Gaussian probability distribution for the values of E_B :

$$P(E_B) = \frac{1}{\sqrt{2\pi}\Delta E_B} \exp\left(-\frac{(E_B - E_{B0})^2}{2\Delta E_B^2}\right). \quad (21)$$

where E_{B0} and ΔE_B were extracted from the experimental spectra. These were the only two adjustable parameters in our treatment. We have found that $E_{B0} - \mu = 0.9 \text{ eV}$ (0.27 eV above E_{c0}), while $\Delta E_B = 0.09 \text{ eV}$

Such an adjustment, however, does not compromise the experimental tests of the theory. The values of E_{B0} and ΔE_B affect the spectral shape but not the integrated noise intensity. Therefore, if the theory predicts a too small noise prefactor, the adjustment of these two parameters only redistributes the spectral intensity in the range of observations but cannot make the theoretical spectra agree with the experimental ones. In the next Section, we shall proceed with an estimate of the prefactor in front of the (approximate) $1/f$ spectral dependence, which is independent of the assumption of the Gaussian shape of $P(E_B)$, but instead relies only on the crude value of $\Delta E_B \sim 0.1$ eV. Since ΔE_B is a characteristic of the energy landscape in a-Si:H, one can hardly expect that it has a much different value. We shall also estimate the integrated noise intensity, which does not depend on the value of ΔE_B at all.

Although the idea that the activation barriers should be distributed is very simple, it has not been exploited previously. One issue here is whether the barriers are long enough or high enough to ensure that the activation processes dominate the tunneling under the potential landscape. Given that not much is reliably known about the random potential landscape on the scale of $1 \div 10$ nm, it is only obvious that the relatively high temperatures of experiment favor the activation processes. From our crude theoretical estimates, the activation over a barrier, which is 0.3 eV high and 3.5 nm, long starts dominating the tunneling under the same barrier at $T = 340K$. For smaller barrier heights or higher temperatures, the critical length of the barrier becomes smaller.

However, our main argument in favor of the existence of the distribution of activation barriers is purely empirical:

The mechanism we describe remains perfectly valid, if one assumes that the activation barriers are not distributed at all, i.e. there exists only one activation barrier for all defects: $E_B = E_{c0}$, and, therefore, $P(E_B) = \delta(E_B - E_{c0})$. In that case, the theoretical spectral intensity predicted by our treatment would significantly exceed the experimental one in the higher frequency part of the observed spectrum at $T = 340K$. One would then have to explain, how another noise mechanism *suppresses* the spectral intensity due to the present one — a task, which seems to be extremely difficult if not impossible.

9. Evaluation of the noise spectrum

Substituting Eq.(19) into Eq.(1) and also using Eq.(20) to switch from integration over τ to integration over E_B , we obtain

$$\frac{S_V(f)}{V^2} = \frac{64\pi^2 e^4 r_s^4 D(\mu)}{\epsilon^2 k_B T V_r} \int_{-\infty}^{+\infty} \frac{\tau(E_B) P(E_B) dE_B}{1 + 4\pi^2 f^2 \tau^2(E_B)} \quad (22)$$

Since the proximity to the $1/f$ spectral shape results only from the fact that the distribution $P(E_B)$ is much broader than $k_B T$, we obtain the prefactor in front of the $1/f$ dependence by substituting the constant value

$$P(E_B) = \frac{1}{2\Delta E_B} \quad (23)$$

into Eq.(22), which gives

$$\frac{S_V(f)}{V^2} \approx \frac{8\pi^2 e^4 r_s^4 D(\mu)}{\epsilon^2 V_r \Delta E_B} \cdot \frac{1}{f} \quad (24)$$

The above estimate cannot be applicable to all frequencies, because Eq.(23) explicitly violates the normalization condition. Nevertheless, expression (24) constitutes a good approximation in a broad frequency domain around the frequency corresponding to the maximum of the probability distribution $P(E_B)$.

One can also obtain the integrated noise intensity (of course, not from the approximation (24) but from Eq.(22)):

$$\int_0^\infty \frac{S_V(f)}{V^2} df \equiv C_V(0) = \frac{16\pi^2 e^4 r_s^4 D(\mu)}{\epsilon^2 k_B T V_r}. \quad (25)$$

If the estimate (15) for $D(\mu)$ is substituted into Eqs.(22,24), then the ‘‘bulk limit’’ results obtained from a more accurate description and reported in Ref. [6] can be recovered.

The remarkable fact about expressions (24,25) is that, even though the noise mechanism rests on the fluctuations of the number of conduction electrons, the resulting spectrum is independent of their equilibrium concentration. Furthermore, the distinct feature of Eq.(24) is that the noise prefactor does not depend on temperature. This should be contrasted with the popular empirical law due to Hooge [24], according to which the noise prefactor is inversely proportional to the number of (thermally activated) carriers and thus decreases exponentially as temperature increases. As far as the defect characteristics are concerned, then the noise intensity depends only on one of them, namely, $D(\mu)$, the density of the defect states at the chemical potential. This dependence is, in fact, weaker than the simple proportionality to $D(\mu)$, and may even exhibit the opposite trend, because deep defects in undoped a-Si:H screen each other, and therefore, the screening radius r_s decreases with the increase of $D(\mu)$ (see Ref. [6]).

10. Comparison with experiment

In Fig. 2, the theoretical spectrum (24) is compared with the experimental ones taken at four different temperatures. The experimental spectra are the same as reported in Ref. [6]. They were obtained by subtracting the zero-current noise from the total noise observed with $V = 50$ meV. The numbers substituted into the theoretical spectrum (24) are the following: $r_s = 0.2 \mu\text{m}$, $\Delta E_B = 0.1$ eV, $\epsilon = 12$, $V_r = z_r A = 0.26 \mu\text{m} \times 0.56 \text{cm}^2$, $D(\mu)$ is obtained from the estimate (15) with $n_D = 6 \cdot 10^{15} \text{cm}^{-3}$ and $\Delta E = 0.15$ eV.

One can observe that (i) the experimental spectra at four different temperatures strongly overlap with each other, in agreement with the temperature independent form of the theoretical expression (24); and (ii) the absolute value of the experimental spectra agree within factor of three with the value given by Eq.(24).

In Fig. 3, we present the comparison between the theoretical (Eq.(25)) and the experimental values of the integrated noise intensity (obtained with the numbers given above). Since the window of experimental observation does not extend over the infinite range of frequencies, we employed the following extrapolation procedure,

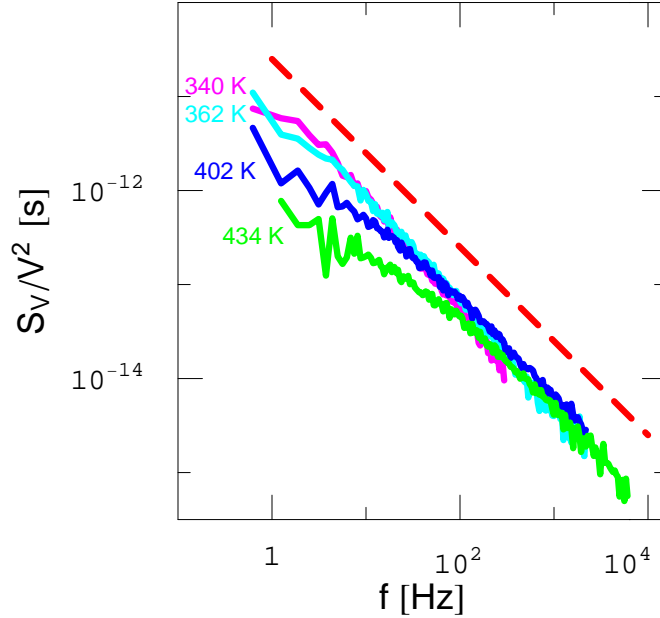


Fig 2. (a) Noise spectra: solid lines represent the experimental data taken at four different temperatures indicated in the plot; dashed line represents the theoretical prediction (24).

which entailed large but quantifiable uncertainties. First, we obtained the lower ends of the error bars by integrating the experimental noise spectra only in the frequency range of the actual experimental observations. Then, the upper ends were obtained by making the power law extrapolations of the spectra beyond the frequency range of observation (up to 10^{-6} Hz for small frequencies and 10^8 Hz for large frequencies), and then adding the integrals over the extrapolated tails to the lower end values of the error bars. Finally, the “experimental” points indicated in Fig. 3 were chosen as the middle points of the above error bars.

Given the relatively crude estimates, which were involved at various stages of the derivation of Eqs.(24,25), and the uncertainty of the values of r_s , $D(\mu)$ and ΔE_B , the agreement is, in fact, very good. In particular, since r_s enters Eqs.(24,25) in the fourth power, the uncertainty in the value of r_s is the single largest source of error in the theoretical predictions. The factor of three discrepancy would vanish if, e.g. $0.15 \mu\text{m}$ were used for r_s instead of $0.2 \mu\text{m}$. In the present case, however, most of the discrepancy can be attributed not to the uncertainty in the value of r_s but to a controllable theoretical error. Namely, the application of the “bulk limit” $r_s \ll z_r$ to the situation, where $r_s \sim z_r$, increases the value of the theoretical noise intensity by factor of two [6]. It has also been shown in Ref. [6] that the calculation *a la* Dutta, Dimon and Horn [4], which uses the Gaussian distribution of energy barriers (Eq.(21)), can account for the temperature-dependent suppression of the noise intensity at the low-frequency end of the experimental spectra.

Finally, we should mention that two additional experimental tests of the present

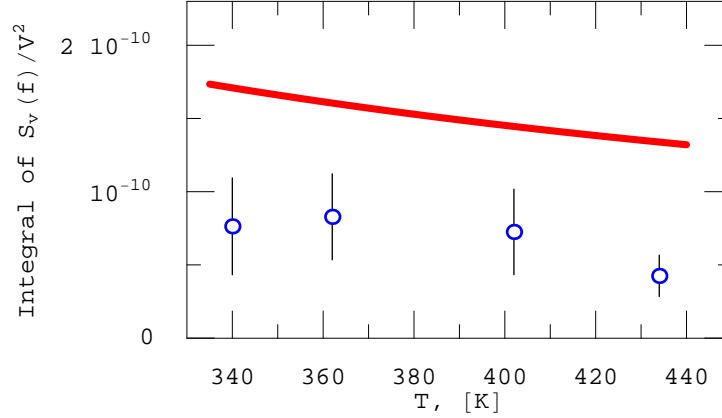


Fig 3. Integrated noise intensity. Empty dots represent the experimental values for the four spectra shown in Fig. 2. The error bars on the experimental points are obtained as described in the text. The solid line corresponds to the theoretical expression (25).

theory, which involve different sandwich structures, are reported by us in an different work [25].

11. Conclusions

In conclusion, we have described a microscopic mechanism of $1/f$ noise in $n-i-n$ sandwich structures of a-Si:H. A very good agreement between this description and our experiments clearly indicates that in the frequency domain $1 - 10^4$ Hz, the noise mechanism proposed is responsible for at least a substantial fraction of the noise intensity observed in experiment. Since this mechanism is quite general, its applicability to a broader class of materials merits further investigation.

ACKNOWLEDGMENTS

We thank R. E. I. Schropp for providing us with the sample. The work of B. V. F. was supported in part by the Netherlands Foundation “Fundamenteel Onderzoek der Materie” (FOM) and the “Nederlandse Organisatie voor Wetenschappelijk Onderzoek” (NWO).

APPENDIX

Here we derive the relationship (10) between small resistivity fluctuations and the resistance fluctuations.

We shall assume that the spatial coarse-graining, which in the following underlies continuous integration, is of the order of $0.01\mu\text{m}$. It is thus much greater than the ballistic mean free path $l_b \approx 5 \div 10\text{\AA}$. Therefore, the electric current flowing through each coarse-grained element can be characterized by Ohm’s law:

$$\mathbf{E}(\mathbf{r}) = \rho(\mathbf{r})\mathbf{j}(\mathbf{r}), \quad (26)$$

where \mathbf{E} is the electric field, ρ the resistivity, \mathbf{j} the current density, and $\mathbf{r} \equiv (x, y, z)$ the position in the sample. The z -axis is chosen along the direction of total current, i.e. perpendicular to the plane of the film.

The potential difference across the resistivity layer is given by integral

$$V = \int_{-z_r/2}^{z_r/2} E_z(x_0, y_0, z) dz = \int_{-z_r/2}^{z_r/2} \rho(x_0, y_0, z) j_z(x_0, y_0, z) dz, \quad (27)$$

where x_0 and y_0 are just two arbitrary coordinates in the plane of the film. In the following, however, we shall use a somewhat redundant but equivalent expression:

$$V = \frac{1}{A} \int_{-z_r/2}^{z_r/2} dz \int_{\mathcal{A}} dx dy \rho(x, y, z) j_z(x, y, z), \quad (28)$$

which represents the average over the equal values of the voltage difference over the area \mathcal{A} of the film.

As a zero approximation, we consider a layer spreading along the z -axis from $-z_r/2$ to $z_r/2$ and having uniform resistivity ρ_0 . We thus represent the total resistivity as

$$\rho(t, \mathbf{r}) = \rho_0 + \delta\rho(t, \mathbf{r}), \quad (29)$$

where $\delta\rho(t, \mathbf{r})$ is a small correction caused by the long-range fluctuations of the local potential

In general, the resistivity fluctuations are accompanied by the fluctuations $\delta\mathbf{j}(t, \mathbf{r})$ of the current density. The expression for the total current density is thus

$$\mathbf{j}(t, \mathbf{r}) = \mathbf{j}_0 + \delta\mathbf{j}(t, \mathbf{r}), \quad (30)$$

where

$$\mathbf{j}_0 = \left(0, 0, \frac{I}{A}\right). \quad (31)$$

The fact, that the total current through the film should stay constant in the presence of the resistance fluctuations, imposes the following constraint:

$$\int_{\mathcal{A}} \delta j_z(t, x, y, z_0) dx dy = 0, \quad (32)$$

where z_0 is an arbitrary coordinate between $-z_r/2$ and $z_r/2$.

Linearizing Eq.(28) with respect to $\delta\rho$ and $\delta\mathbf{j}$ we obtain

$$\delta V(t) = \frac{1}{A} \int_{\mathcal{V}} [\delta\rho(t, \mathbf{r}) j_{0z} + \rho_0 \delta j_z(t, \mathbf{r})] dx dy dz, \quad (33)$$

where \mathcal{V} refers to the three-dimensional space limited by $\pm z_r/2$ along the z axis and by the edges of the film in the xy -plane. The integration of the second term in Eq.(33) gives zero by virtue of constraint (32). Thus, recalling that $j_{0z} = I/A$, we obtain Eq.(10)

$$\delta R(t) = \frac{\delta V(t)}{I} = \frac{1}{A^2} \int_{\mathcal{V}} \delta\rho(t, \mathbf{r}) d^3r. \quad (34)$$

References

- [1] R. A. Street, *Hydrogenated amorphous silicon*, Cambridge University Press, Cambridge, 1991.
- [2] A. van der Ziel, *Physica (Utrecht)* **16**, p. 359, 1950.
- [3] F. K. du Pre, *Phys. Rev.* **78**, p. 615, 1950.
- [4] P. Dutta, P. Dimon, and P. M. Horn, *Phys. Rev. Lett.* **43**, p. 646, 1979.
- [5] M. B. Weissman, *Rev. Mod. Phys.* **60**, p. 537, 1988.
- [6] B. V. Fine, J. P. R. Bakker, and J. I. Dijkhuis, *Phys. Rev. B* **68**, p. 125207, 2002. eprint cond-mat/0210680.
- [7] P. A. W. E. Verleg and J. I. Dijkhuis, *Phys. Rev. B* **58**, p. 3904, 1998.
- [8] F. Z. Bathaei and J. C. Anderson, *Philos. Mag. B* **55**, p. 87, 1987.
- [9] M. Baciocchi, A. D'Amico, and C. Vliet, *Solid-St. Electron.* **34**, p. 1439, 1991.
- [10] C. E. Parman and J. Kakalios, *Phys. Rev. Lett.* **67**, p. 2529, 1991.
- [11] C. E. Parman, N. E. Israeloff, and J. Kakalios, *Phys. Rev. B* **44**, p. 8391, 1991.
- [12] G. M. Khera and J. Kakalios, *Phys. Rev. B* **56**, p. 1918, 1997.
- [13] P. A. W. E. Verleg and J. I. Dijkhuis, *Phys. Rev. B* **58**, p. 3917, 1998.
- [14] M. Günes, R. Johanson, and S. Kasap, *Phys. Rev. B* **60**, p. 1477, 1999.
- [15] S. T. B. Goennenwein *et al.*, *Phys. Rev. Lett.* **84**, p. 5188, 2000.
- [16] R. E. Johanson *et al.*, *J. Vac. Sci. Technol. A* **18**, p. 661, 2000.
- [17] J. P. R. Bakker, *Ph. D. thesis, University of Utrecht*, 2003.
- [18] J. P. R. Bakker, P. J. S. van Capel, B. V. Fine, and D. I. Dijkhuis, *MRS Proceedings* **715**, p. A2.6, 2002.
- [19] L. M. Lust and J. Kakalios, *Phys. Rev. Lett.* **75**, p. 2192, 1995.
- [20] J. B. Johnson, *Phys. Rev.* **32**, p. 97, 1928.
- [21] H. Nyquist, *Phys. Rev.* **32**, p. 110, 1928.
- [22] S. O. Kasap, M. Gunes, R. E. Johanson, Q. Wang, Y. Yang, and S. Guha, *J. Mater. Sci.: Materials in Electronics* **14**, pp. 693–696, 2003.
- [23] T. J. Belich and J. Kakalios, *Phys. Rev. B* **66**, p. 195212, 2002.
- [24] F. N. Hooge, *Phys. Lett. A* **29**, p. 139, 1969.
- [25] J. P. R. Bakker, P. J. S. van Capel, B. V. Fine, and J. I. Dijkhuis, *J. Non-Cryst. Solids* **338-340**, p. 310, 2004. eprint cond-mat/0310468.